Positive- and negative-effective-viscosity phenomena in isotropic and anisotropic Beltrami flows

B. J. Bayly and V. Yakhot
Program in Applied and Computational Mathematics, Princeton University, Fine Hall, Princeton, New Jersey 08544
(Received 23 December 1985)

A field-theoretic approach, analogous to Kraichnan's direct-interaction approximation, to the stability theory of complex three-dimensional flows is developed. The long-wavelength stability of a class of Beltrami flows in an unbounded, viscous fluid is considered. We examine two flows in detail, to illustrate the effects of strong isotropy versus strong anisotropy in the basic flow. The effect of the small-scale flow on the long-wavelength perturbations may be interpreted as an effective viscosity. Using diagrammatic techniques, we construct the first-order smoothing and direct-interaction approximations for the perturbation dynamics. It is argued that the effective viscosity for the isotropic flow is always positive, and approaches a value independent of the molecular viscosity in the high-Reynolds-number limit; this flow is thus stable to long-wavelength disturbances. The anisotropic flow has negative effective viscosity for some orientations of the disturbance, and is therefore unstable, when its Reynolds number exceeds $\sqrt{2}$.

I. INTRODUCTION

One of the most intriguing problems in the theory of hydrodynamic turbulence is the formation of large-scale structures in a liquid performing random (turbulent) motion at small scales. It is natural to explain the spontaneous formation of large-scale structures as a manifestation of a long-wavelength instability of the corresponding small-scale flow. In a theoretical approach to the description of this phenomenon, it is convenient to assume that the small-scale flow is driven by an external force field which varies with respect to the space coordinates. A previous paper[1] treated the long-wavelength stability of two-dimensional, periodic eddy systems, driven by appropriate steady forces; it was shown that the large-scale instability is likely to occur only if the small-scale flow is sufficiently anisotropic.

In this paper we shall consider small-scale flows of the following form:

$$\bar{\mathbf{v}}(\mathbf{x})=\sum_{\hat{\mathbf{Q}}\in W} A(\hat{\mathbf{Q}})(\hat{\mathbf{n}}+i\hat{\mathbf{Q}}\times\hat{\mathbf{n}})e^{i\hat{\mathbf{Q}}\cdot\mathbf{x}/L}\,, \tag{1.1}$$

where W is a finite set of unit vectors which contains $-\hat{\mathbf{Q}}$ whenever it contains $\hat{\mathbf{Q}}$. The velocity field is guaranteed to be real by requiring that the Fourier amplitudes A satisfy $A(-\hat{\mathbf{Q}})=A^*(\hat{\mathbf{Q}})$ for each $\hat{\mathbf{Q}}\in W$. The vector $\hat{\mathbf{n}}$ is a unit vector orthogonal to $\hat{\mathbf{Q}}$. For our purposes it is unnecessary to specify just which vector $\hat{\mathbf{n}}$ is chosen out of the unit circle of candidates; changing the choice of $\hat{\mathbf{n}}$ is equivalent to changing the phase of the corresponding amplitude A, which turns out to be irrelevant to the long-wavelength stability results. $2\pi L$ is the fundamental period of each Fourier component.

The flows (1.1) have the particular property that the vorticity vector is everywhere a constant scalar multiple of the velocity vector (we shall call this the strong Beltrami property, as opposed to the weak Beltrami property, in which the vorticity is a nonconstant scalar multiple of the velocity). This means that the nonlinear term in the Navier-Stokes equations reduces to the gradient of a scalar, which can be absorbed into the pressure field. Thus, any velocity field of the form (1.1) is a nontrivial exact steady solution of the Euler equations. Alternatively, we can think of the flow (1.1) as an exact steady flow of a viscous fluid maintained by an externally imposed body force $\mathbf{f}=(\rho\nu/L^2)\bar{\mathbf{v}}$, where ν is the kinematic viscosity of the fluid.

From the class (1.1) of Beltrami flows, we shall select two for explicit calculations. To observe the effects of extreme anisotropy in the basic state, we shall consider the simple flow obtained when W contains only two wave vectors $\pm\hat{\mathbf{Q}}$, which can be chosen to be $(\pm1,0,0)$. With the choice $\hat{\mathbf{n}}=(0,1,0)$ and real amplitude $A(\pm\hat{\mathbf{Q}})=U_{\rm rms}/2$, the flow is

$$\bar{\mathbf{v}}=U_{\rm rms}(0,\cos(x/L),-\sin(x/L))\,, \tag{1.2}$$

which has the form of a monochromatic, circularly polarized wave. For the opposite extreme of highly isotropic flow, let us choose W to consist of a large number N of unit vectors $\hat{\mathbf{Q}}$ distributed isotropically over the unit sphere. The complex amplitudes $A(\hat{\mathbf{Q}})$ are all given modulus $U_{\rm rms}/\sqrt{2N}$; the phases of $A(\hat{\mathbf{Q}})$ are immaterial, and may be chosen randomly. In either case, $U_{\rm rms}$ is the root-mean-square fluid velocity, and is held fixed as N is varied to obtain different degrees of isotropy. Beltrami flows of this type have been used extensively in simulations of diffusion in helical turbulence,[4] but the present work appears to be the first investigation of their dynamical properties.

The possibility that a small-scale flow with nonzero average helicity might be unstable to the growth of long-wavelength disturbances has been discussed by a number of authors. Moffatt[5] has shown that a certain very symmetric Beltrami flow with six Fourier components, known as the Arnol'd-Beltrami-Childress (ABC) flow, is inviscidly unstable to large-scale disturbances with the same sign

of helicity (i.e., the same "handedness") as the basic flow, and Moissev *et al.*[6] have shown that, in a highly compressible fluid, any small-scale turbulent flow with nonzero helicity can support a growing large-scale secondary flow. The purpose of the present paper is to perform an investigation of the possibility of long-wave instability in viscous, incompressible flow, which is typically the situation of greatest physical interest. It is our suspicion that under these conditions, most nontrivial Beltrami flows are stable, and as such may occur and persist in a large variety of turbulent flows.[7,8]

In this paper, we consider the behavior of long-wavelength disturbances to viscous Beltrami flows, which we assume are maintained by steady external body forces. The perturbation is expanded in powers of the Reynolds number of the basic flow, and we evaluate each term in the long-wave limit. This expansion is essentially the same as the expansion for the long-wave behavior of the averaged impulse-response tensor in a fully turbulent flow, for which Kraichnan originally developed the so-called direct-interaction approximation (DIA). The DIA, as usually used in turbulence theory, consists of an equation for the impulse-response tensor, coupled with an equation giving the evolution of the velocity-velocity correlation function. In this paper, the basic flow is known exactly, so we do not need the auxiliary equation for the velocity autocorrelation. The resulting system is considerably simpler to analyze than most applications of the DIA. We construct both the first-order smoothing and direct-interaction approximations and examine their implications for the two flows described above.

In the long-wave approximation, the growth or decay rate of a large-scale perturbation is a quadratic function of the wave number of the perturbation. For this reason, the effect of the small-scale flow on the evolution of long-wave disturbances may be interpreted as the action of a tensor effective viscosity. In the case of the simple Beltrami flow (1.2) with two Fourier components, only the first nontrivial diagram survives in the long-wave limit for any finite Reynolds number, and the first-order smoothing approximation correctly determines the exact evolution of large-scale perturbations. The effective viscosity is anisotropic, and is actually negative for some orientations of the perturbation. It turns out that large-scale perturbations of suitable orientation are capable of growing on the flow (1.2) when its Reynolds number exceeds $\sqrt{2}$.

For almost isotropic Beltrami flows at low Reynolds numbers, first-order smoothing theory indicates that the viscous damping of long-wave disturbances is enhanced by the reaction of the basic flow, the effective viscosity being isotropic and positive in this case. At finite Reynolds number, however, all terms in the expansion are nominally of the same order in the long-wave limit, and first-order smoothing no longer remains applicable. The solution of the direct-interaction approximation for these flows indicates that the effective viscosity increases with the Reynolds number, eventually approaching a value independent of the molecular viscosity in the limit of infinite Reynolds number. This result supports the conjecture that a large class of Beltrami flows with nontrivial topologies are stable, and might be observed in experiments or numerical simulations.

II. FORMULATION OF THE LONG-WAVE STABILITY PROBLEM

The equations of motion for a viscous fluid in the presence of a steady, quasiperiodic force field are most conveniently used in dimensionless form. Using L as the length scale and ν/L as the velocity scale, the dimensionless Navier-Stokes equations take the form

$$\begin{aligned} &\mathbf{v}_t + R\mathbf{v}\cdot\nabla\mathbf{v} = -\nabla p + \nabla^2\mathbf{v} + \mathbf{f} , \\ &\nabla\cdot\mathbf{v} = 0 , \end{aligned} \tag{2.1}$$

where

$$\mathbf{f}(\mathbf{x}) = \sum_{\hat{\mathbf{Q}}\in W} \mathbf{F}(\hat{\mathbf{Q}}) e^{i\hat{\mathbf{Q}}\cdot\mathbf{x}} , \quad \mathbf{F}(\hat{\mathbf{Q}}) = A(\hat{\mathbf{Q}})(\hat{\mathbf{n}} + i\hat{\mathbf{Q}}\times\hat{\mathbf{n}}) , \tag{2.2}$$

and the $|A(\hat{\mathbf{Q}})|$, now dimensionless, have been scaled with respect to the root-mean-square fluid velocity $U_{\rm rms}$. R is the Reynolds number based on $U_{\rm rms}$, L, and ν. Henceforth, unless explicitly stated, we shall work exclusively with the nondimensional quantities as defined here.

If we define the four-dimensional Fourier transforms of space-time–dependent quantities by

$$\begin{aligned} a(\mathbf{k},\omega) &\equiv \int \frac{d\mathbf{x}\,dt}{(2\pi)^4} e^{-i(\mathbf{k}\cdot\mathbf{x}-\omega t)} a(\mathbf{x},t) , \\ a(\mathbf{x},t) &\equiv \int d\mathbf{k}\,d\omega\, e^{i(\mathbf{k}\cdot\mathbf{x}-\omega t)} a(\mathbf{k},\omega) , \end{aligned} \tag{2.3}$$

then we can write the Navier-Stokes equations as

$$\begin{aligned} v_i(\mathbf{k},\omega) = {} & G^0(\mathbf{k},0) f_i(\mathbf{k})\delta(\omega) \\ & + G^0(\mathbf{k},\omega)(-\tfrac{1}{2}iR) P_{ijl}(\mathbf{k}) \\ & \times \int d\mathbf{q}\,d\sigma\, v_j(\mathbf{q},\sigma) v_l(\mathbf{k}-\mathbf{q},\omega-\sigma) . \end{aligned} \tag{2.4}$$

Here $G^0(\mathbf{k},\omega) \equiv (-i\omega + k^2)^{-1}$ is the so-called zero-order propagator, and

$$P_{ijl}(\mathbf{k}) \equiv k_j(\delta_{il} - k_i k_j/k^2) + k_l(\delta_{ij} - k_i k_l/k^2) .$$

The tensor P_{ijl} incorporates the pressure field and the incompressibility constraint, allowing us to replace the two equations (2.1) by only one (2.4).

The Fourier transform of the force is a sum of δ functions:

$$f_i(\mathbf{k}) = \sum_{\hat{\mathbf{Q}}\in W} F_i(\hat{\mathbf{Q}})\delta(\mathbf{k}-\hat{\mathbf{Q}}) . \tag{2.5}$$

The Beltrami property of the basic flow implies that the nonlinear term

$$P_{ijl}(\mathbf{k}) \int d\mathbf{q} f_j(\mathbf{q}) f_l(\mathbf{k}-\mathbf{q}) \tag{2.6}$$

vanishes identically, and the basic flow therefore takes the form

$$\mathbf{v}(\mathbf{k}) = G^0(\mathbf{k},0)\mathbf{f}(\mathbf{k})\delta(\omega) .$$

To investigate the stability of the basic state, we imagine an infinitesimal perturbation $v_i'(\mathbf{k},\omega)$ to the flow

$$v_i(\mathbf{k},\omega)=G^0(\mathbf{k},0)f_i(\mathbf{k})\delta(\omega)+v_i'(\mathbf{k},\omega) \tag{2.7}$$

and consider its evolution according to the linearized equation

$$v_a'(\mathbf{k},\omega)=G^0(\mathbf{k},\omega)(-iR)P_{abc}(\mathbf{k}) \times \int d\mathbf{q}\, G^0(\mathbf{q},0)f_b(\mathbf{q})v_c'(\mathbf{k}-\mathbf{q},\omega) . \tag{2.8}$$

Because of the coupling between the perturbation and the small-scale basic flow, a pure long-wave perturbation is impossible, but we can formally separate the perturbation into long-and short-wave components:

$$v_a'(\mathbf{k},\omega)=v_a^<(\mathbf{k},\omega)+v_a^>(\mathbf{k},\omega) , \tag{2.9}$$

where

$$v_a^<(\mathbf{k},\omega)\equiv 0 \text{ if } |\mathbf{k}|>\epsilon , \qquad v_a^>(\mathbf{k},\omega)\equiv 0 \text{ if } |\mathbf{k}|<\epsilon , \tag{2.10}$$

for some long-wave cutoff $0<\epsilon\ll 1$. We define the operators $\langle\ \rangle$ and $I-\langle\ \rangle$ as the projections onto the long- and short-wave subspaces, respectively, of the function space we are working in.

The long- and short-wave projections of the equation of motion (2.8) are then

$$v_a^<(\mathbf{k},\omega)=G^0(\mathbf{k},\omega)(-iR)P_{abc}(\mathbf{k})\int d\mathbf{q}G^0(\mathbf{q},0)\langle f_b(\mathbf{q})v_c^>(\mathbf{k}-\mathbf{q},\omega)\rangle , \tag{2.11a}$$

$$v_c^>(\mathbf{k},\omega)=G^0(\mathbf{k},\omega)(-iR)P_{cde}(\mathbf{k})\int d\mathbf{q}\, G^0(\mathbf{q},0)f_d(\mathbf{q})v_e^<(\mathbf{k}-\mathbf{q},\omega) +G^0(\mathbf{k},\omega)(-iR)P_{cde}(\mathbf{k})\int d\mathbf{q}\, G^0(\mathbf{q},0)[f_d(\mathbf{q})v_e^>(\mathbf{k}-\mathbf{q},\omega)-\langle f_d(\mathbf{q})v_e^>(\mathbf{k}-\mathbf{q},\omega)\rangle] . \tag{2.11b}$$

The short-wave component can be expressed in terms of the long-wave component by formally iterating (2.11b), which yields an expression in the form of a perturbation series in powers of the Reynolds number of the basic flow. When this series substituted into (2.11a), we obtain an equation involving only the long-wave component of the perturbation, which determines the evolution of the entire perturbation. The analysis of this equation occupies the rest of the paper.

III. FIRST-ORDER SMOOTHING

The first-order smoothing approximation consists of taking only one iteration of the short-wave equation (2.11b) before substituting the result back into the long-wave equation. This amounts to taking the first term in the Reynolds-number expansion of the evolution equation, so the results will be strictly valid only for small Reynolds number. In this regime, the molecular viscosity dominates the inertial processes, so all disturbances are damped. Nevertheless, we can observe whether the small-scale flow tends to enhance or diminish the dissipation, and this information will give us some indication of the situation at higher Reynolds numbers.

The first iteration of (2.11b) yields

$$v_c^>(\mathbf{k},\omega)=G^0(\mathbf{k},\omega)(-iR)P_{cde}(\mathbf{k})\int d\mathbf{q}\, G^0(\mathbf{q},0)f_d(\mathbf{q})v_e^<(\mathbf{k}-\mathbf{q},\omega) . \tag{3.1}$$

Substituting into (2.11a) then gives an appropriate equation of motion for the long-wave component alone:

$$\begin{aligned} v_a^<(\mathbf{k},\omega)&=G^0(\mathbf{k},\omega)(-iR)P_{abc}(\mathbf{k})\int d\mathbf{q}^1 G^0(\mathbf{q}^1,0)f_b(\mathbf{q}^1)G^0(\mathbf{k}-\mathbf{q}^1,\omega)(-iR)P_{cde}(\mathbf{k}-\mathbf{q}^1) \\ &\quad\times\int d\mathbf{q}^2 G^0(\mathbf{q}^2,0)f_d(\mathbf{q}^2)v_e^<(\mathbf{k}-\mathbf{q}^1-\mathbf{q}^2) \\ &=-R^2G^0(\mathbf{k},\omega)P_{abc}(\mathbf{k})\sum_{\hat{\mathbf{Q}}^1,\hat{\mathbf{Q}}^2\in W} G^0(\mathbf{k}-\hat{\mathbf{Q}}^1,\omega)P_{cde}(\mathbf{k}-\hat{\mathbf{Q}}^1)F_b(\hat{\mathbf{Q}}^1)F_d(\hat{\mathbf{Q}}^2)v_e^<(\mathbf{k}-\hat{\mathbf{Q}}^1-\hat{\mathbf{Q}}^2,\omega) \end{aligned} \tag{3.2}$$

after performing the q integrals. But $v_e^<(\mathbf{k}-\hat{\mathbf{Q}}^1-\hat{\mathbf{Q}}^2,\omega)$ is nonzero only if $\hat{\mathbf{Q}}^2=-\hat{\mathbf{Q}}^1+O(\epsilon)$, which implies $\hat{\mathbf{Q}}^2=-\hat{\mathbf{Q}}^1$, because there is only a finite number of distinct wave vectors in W and we are interested in the limit $\epsilon\to 0$. Therefore,

$$v_a^<(\mathbf{k},\omega)=-R^2G^0(\mathbf{k},\omega)P_{abc}(\mathbf{k})\sum_{\hat{\mathbf{Q}}\in W} G^0(\mathbf{k}-\hat{\mathbf{Q}})P_{cde}(\mathbf{k}-\hat{\mathbf{Q}})|A(\hat{\mathbf{Q}})|^2(\delta_{bd}-\hat{Q}_b\hat{Q}_d-i\epsilon_{bdx}\hat{Q}_x)v_e^<(\mathbf{k},\omega) , \tag{3.3}$$

where we have used the fact that a helical vector $\mathbf{F}(\hat{\mathbf{Q}})=A(\hat{\mathbf{Q}})[\hat{\mathbf{n}}+i\hat{\mathbf{Q}}\times\hat{\mathbf{n}}]$ has the property that

$$F_b(\hat{\mathbf{Q}})F_d(-\hat{\mathbf{Q}})=|A(\hat{\mathbf{Q}})|^2(\delta_{db}-\hat{Q}_b\hat{Q}_d-i\epsilon_{bdx}\hat{Q}_x) , \tag{3.4}$$

regardless of the phase of $A(\hat{\mathbf{Q}})$ or the choice of $\hat{\mathbf{n}}$.

Now, we can simplify (3.3) by taking the limit of small $|\mathbf{k}|$ and using the incompressibility conditions

$$\hat{Q}_aF_a(\hat{\mathbf{Q}})=0 , \quad k_av_a^<(\mathbf{k},\omega)=0 . \tag{3.5}$$

First, consider

$$P_{cde}(\mathbf{k}-\hat{\mathbf{Q}})=(k_d-\hat{Q}_d)\left[\delta_{ce}\frac{(k_c-\hat{Q}_c)(k_e-\hat{Q}_e)}{|\mathbf{k}-\hat{\mathbf{Q}}|^2}\right]+(k_e-\hat{Q}_e)\left[\delta_{cd}-\frac{(k_c-\hat{Q}_c)(k_d-\hat{Q}_d)}{|\mathbf{k}-\hat{\mathbf{Q}}|^2}\right].$$

Any term containing $\hat{Q}_d$ vanishes on contraction with $(\delta_{bd}-\hat{Q}_b\hat{Q}_d-i\epsilon_{bdx}\hat{Q}_x)$, and any term containing k_e vanishes on contraction with $v_e^<(\mathbf{k},\omega)$, therefore the only important part of $P_{cde}(\mathbf{k}-\hat{\mathbf{Q}})$ is

$$-\hat{Q}_e\delta_{cd}+k_d(\delta_{ce}-2\hat{Q}_c\hat{Q}_e)+O(k^2)\,. \tag{3.6}$$

The leading-order contribution (in k) to the right-hand side of (3.3) is

$$G^0(\mathbf{k})P_{abc}(\mathbf{k})\sum_{\hat{\mathbf{Q}}\in W}|A(\hat{\mathbf{Q}})|^2(-\hat{Q}_e\delta_{cd})(\delta_{bd}-\hat{Q}_b\hat{Q}_d-i\epsilon b_{dx}\hat{Q}_x)v_e^<(\mathbf{k},\omega)\,. \tag{3.7}$$

Now, $(\delta_{bd}-\hat{Q}_b\hat{Q}_d)(-\hat{Q}_e)$ is odd in $\hat{\mathbf{Q}}$, and thus gives no contributions when summed over all $\hat{\mathbf{Q}}$. Also, $(-\hat{Q}_e\delta_{cd})(-i\epsilon_{bdx}\hat{Q}_x)$ is antisymmetric in b,c, and vanishes upon contradiction with $P_{abc}(\mathbf{k})$. Therefore, the dominant behavior of the right-hand side of (3.3) is quadratic in $|\mathbf{k}|$, and may be interpreted as an effective eddy viscosity acting on $v_e^<$.

To go to the next order in $|\mathbf{k}|$, we need to correct the propagator

$$G^0(\mathbf{k}-\hat{\mathbf{Q}},\omega)=1+2k_i\hat{Q}_i+O(k^2)\,, \tag{3.8}$$

anticipating that ω will turn out to be quadratic in $\mathbf{k}$. To order k^2, then, (3.3) is

$$v_a^<(\mathbf{k},\omega)=-R^2G^0(\mathbf{k})P_{abc}(\mathbf{k})v_e^<(\mathbf{k},\omega)\sum_{\hat{\mathbf{Q}}\in W}|A(\hat{\mathbf{Q}})|^2[2k_i\hat{\mathbf{Q}}_i(-\hat{Q}_e\delta_{cd})(\delta_{bd}-\hat{Q}_b\hat{Q}_d-\epsilon_{bdx}\hat{Q}_x)$$
$$+k_d(\delta_{ce}-2\hat{Q}_c\hat{Q}_e)(\delta_{bd}-\hat{Q}_b\hat{Q}_d-i\epsilon_{bdx}\hat{Q}_x)]\,. \tag{3.9}$$

The terms proportional to $\epsilon_{bdx}\hat{Q}_x$ are odd in $\hat{\mathbf{Q}}$ and vanish in the sum, leaving

$$v_a^<(\mathbf{k},\omega)=-R^2G^0(\mathbf{k},\omega)P_{abc}(\mathbf{k})k_dv_e^<(\mathbf{k},\omega)$$
$$\times\sum_{\hat{\mathbf{Q}}\in W}|A(\hat{\mathbf{Q}})|^2(\delta_{ce}\delta_{bd}-2\delta_{bd}\hat{Q}_c\hat{Q}_e-\delta_{ce}\hat{Q}_b\hat{Q}_d-2\delta_{bc}\hat{Q}_d\hat{Q}_e+4\hat{Q}_b\hat{Q}_c\hat{Q}_d\hat{Q}_e)\,. \tag{3.10}$$

Let us now consider the simple flow (1.2), with only two Fourier components. Choosing the perturbation wave vector to be $\mathbf{k}=(0,k,0)$, (3.10) becomes

$$v_1^<(\mathbf{k},\omega)=\tfrac{1}{2}R^2G^0(\mathbf{k},\omega)k^2v_1^<(\mathbf{k},\omega)\,, \tag{3.11a}$$

$$v_3^<(\mathbf{k},\omega)=-\tfrac{1}{2}R^2G^0(\mathbf{k},\omega)k^2v_3^<(\mathbf{k},\omega)\,, \tag{3.11b}$$

whence

$$-i\omega v_1^<(\mathbf{k},\omega)=-k^2(1-\tfrac{1}{2}R^2)v_1^<(\mathbf{k},\omega)\,, \tag{3.12a}$$

$$-i\omega v_3^<(\mathbf{k},\omega)=-k^2(1+\tfrac{1}{2}R^2)v_3^<(\mathbf{k},\omega)\,. \tag{3.12b}$$

The small-scale flow thus has a stabilizing effect on the large-scale flow orthogonal to the basic-flow wave vectors, and a destabilizing effect on the large-scale flow when it is aligned with the basic-flow wave vectors. Indeed, this result suggests that small-scale flow will be unstable when the Reynolds number, as defined here, exceeds $\sqrt{2}$.

In order to evaluate (3.10) for an almost-isotropic flow with many Fourier components, it is hopeless to perform the sum exactly, particularly if we want to obtain results applicable to a large class of flows. Therefore, we shall replace the sum in (3.10) with an integral over the unit sphere, and obtain an exactly isotropic equation which will approximate the dynamics of perturbations on the large class of almost-isotropic flows. Since the root-mean-square velocity was used in scaling the dimensionless equations, the sums in (3.10) have the numerical values

$$\sum_{S^2}|A(\hat{\mathbf{Q}})|^2=1\,,$$
$$\sum_{S^2}|A(\hat{\mathbf{Q}})|^2\hat{Q}_i\hat{Q}_j=\tfrac{1}{3}\delta_{ij}\,, \tag{3.13}$$
$$\sum_{S^2}|A(\hat{\mathbf{Q}})|^2\hat{Q}_i\hat{Q}_j\hat{Q}_k\hat{Q}_l=\tfrac{1}{15}(\delta_{ij}\delta_{kl}+\delta_{ik}\delta_{jl}+\delta_{il}\delta_{jk})\,.$$

All the terms in (3.10) containing δ tensors either cancel or vanish due to incompressibility, therefore,

$$v_a^<(\mathbf{k},\omega)=-R^2G^0(\mathbf{k},\omega)P_{abc}(\mathbf{k})k_dv_e^<(\mathbf{k},\omega)$$
$$\times\tfrac{4}{15}(\delta_{bc}\delta_{de}+\delta_{bd}\delta_{ce}+\delta_{be}\delta_{cd})$$
$$=-R^2G^0(\mathbf{k},\omega)\tfrac{8}{15}k^2v_a^<(\mathbf{k},\omega)\,. \tag{3.14}$$

All long-wave disturbances are uniformly damped, with decay rate given by

$$-i\omega = -k^2(1+\tfrac{8}{15}R^2) . \tag{3.15}$$

The small-scale flow in this case therefore enhances the damping of all long-wave disturbances irrespective of wave-vector direction or polarization, as would be anticipated for such an isotropic small-scale flow. In particular, the isotropic nature of the small-scale flow has eliminated the special directions in which perturbations were amplified or only weakly damped.

IV. HIGHER-ORDER THEORY: DIAGRAM EXPANSION AND DIA

Because of the complexity of the algebraic manipulations, we shall use diagrammatic notation for analyzing the perturbation equations (2.11). The procedure is standard, but we shall present the derivations in detail for the sake of completeness. Let the thin line represent the zero order propagator G^0, the cross denote the force f, and the vertex the quantity $(-iR)P$, with indices to be specified later. Also, let the open bar represent the long-wave part of the perturbation, and the slashed open bar the short-wave part. These symbols are drawn in Figs. 1(a)–1(e), respectively.

Equations (2.11a) and (2.11b) can then be represented by the diagrams in Figs. 2(a) and 2(b). Each vertex has a line exiting on the left, a line entering from the right, and a line entering from the upper right, whose other end consists of a force term. Each of these lines possesses a wave vector and an index, which must agree with the wave vector and index at the force or vertex at each of its ends. At each vertex, the wave vector on the left must equal the sum of the right wave vector and the slanted force wave vector. All repeated indices are summed over, and all internal wave vectors are integrated, resulting in wave-vector sums of the same form as (2.13). Since the vertex

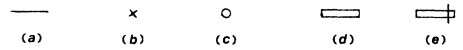

FIG. 1. Constituents of diagrams.

contains a factor of the Reynolds number, a diagram with n vertices corresponds to a quantity proportional to R^n.

The short-wave perturbation may be expressed in terms of the long-wave part by iterating Fig. 2(b). The first two approximations are shown in Fig. 3. Now, the term a in Fig. 3 translates into the algebraic expression

$$-R^2 \sum_{\hat{\mathbf{Q}}^1,\hat{\mathbf{Q}}^2 \in W} P_{abc}(\mathbf{k})G^0(\hat{\mathbf{Q}}^1)F_b(\hat{\mathbf{Q}}^1)G^0(\mathbf{k}-\hat{\mathbf{Q}}^1) \times P_{cde}(\mathbf{k}-\hat{\mathbf{Q}}^1)G^0(\hat{\mathbf{Q}}^2)F_d(\hat{\mathbf{Q}}^2)v_e^<(\mathbf{k}-\hat{\mathbf{Q}}^1-\hat{\mathbf{Q}}^2,\omega)$$

and so the only contribution to the long-wave projection b of term a comes from pairs $\hat{\mathbf{Q}}^1,\hat{\mathbf{Q}}^2$ that cancel. This can be indicated diagrammatically by replacing the force branches by an arc as in Fig. 4(a).

In general, the long-wave part of a diagram with an odd number of force branches vanishes, and the long-wave part of a diagram with an even number of branches is the sum of all possible diagrams obtained by connecting the branches in pairs. For example, the long-wave parts of the next nontrivial diagram is shown in Fig. 4(b). Long-wave diagrams that can be disconnected by severing one G^0 line are called *reducible* diagrams (labeled r in Fig. 4), and those which cannot (labeled i) are *irreducible*. So as not to count diagrams with internal wave vector $\mathbf{k}$ twice, we require the following rule for evaluating irreducible diagrams: the sum over all wave-vector combinations must exclude those for which one (or more) of the internal wave vectors is $\mathbf{k}$. So, for instance, the diagram in Fig. 4(c) with the crossed arcs has the value

$$R^4 \sum_{\hat{\mathbf{Q}}^2 \neq -\hat{\mathbf{Q}}^1} G^0(\mathbf{k},\omega)P_{abc}(\mathbf{k})F_b(\hat{\mathbf{Q}}^1)G^0(\mathbf{k}-\hat{\mathbf{Q}}^1,\omega)P_{cde}(\mathbf{k}-\hat{\mathbf{Q}}^1)F_d(\hat{\mathbf{Q}}^2) \times G^0(\mathbf{k}-\hat{\mathbf{Q}}^1-\hat{\mathbf{Q}}^2,\omega)P_{efi}(\mathbf{k}-\hat{\mathbf{Q}}^1-\hat{\mathbf{Q}}^2)F_f(-\hat{\mathbf{Q}}^1)G^0(\mathbf{k}-\hat{\mathbf{Q}}^2,\omega)P_{ijm}(\mathbf{k}-\hat{\mathbf{Q}}^2)F_j(-\hat{\mathbf{Q}}^2)v_m^<(\mathbf{k},\omega) .$$

We can now extend the iteration scheme for $v_i^>(\mathbf{k},\omega)$ to arbitrary order in R. The next approximations are shown in Fig. 5. The two reducible diagrams in Fig. 5(b) cancel, leaving an expression for the fourth approximation that involves only irreducible diagrams. This cancellation of reducible diagrams is quite general, and the full expansion of $v_i^>(\mathbf{k},\omega)$ is given in Fig. 6. The quantity I_m is the sum of all irreducible diagrams with $2m$ vertices, minus the external legs.

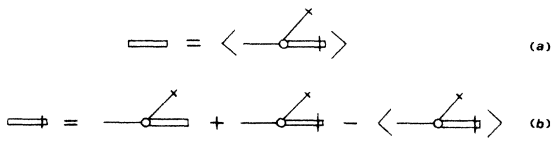

FIG. 2. Equation (2.11) in diagram form.

Having found the expansion of $v_i^>$ in terms of $v_i^<$ we can now substitute it into Fig. 2(a) to find the equation of motion for $v_i^<$ by itself. Only the diagrams in Fig. 6 with an odd number of branches contribute, and all the reducible diagrams cancel in the long-wave projection, leaving the expression in Fig. 7(a). Figure 7(a) can be rewritten in terms of the renormalized vertex $\Sigma_{ab}(\mathbf{k},\omega)$, defined as the sum of all the legless irreducible diagrams. The resulting equation [Fig. 7(b)], whose algebraic translation is

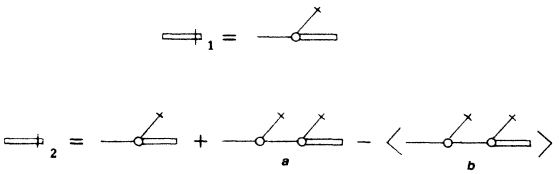

FIG. 3. First two iterations of Fig. 2(b).

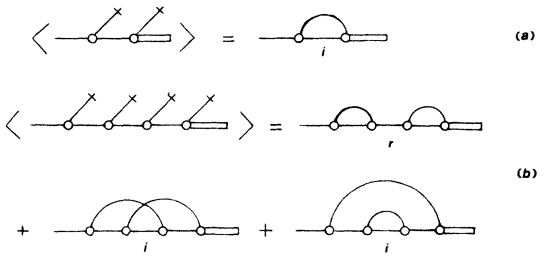

FIG. 4. Long-wave components of simple diagrams.

$$v_a^<(\mathbf{k},\omega)=G^0(\mathbf{k},\omega)\Sigma_{ab}(\mathbf{k},\omega)v_b^<(\mathbf{k},\omega)\ , \tag{4.1}$$

can then be solved provided we can find some sensible approximation for $\Sigma_{ab}(\mathbf{k},\omega)$.

Formally, therefore, we have found the exact form of the Reynolds-number expansion of the long-wave equation of motion. Strictly speaking, the expansion procedure is only valid when $R \ll 1$, in which case we can get a good approximation to the dynamics by taking only the first term in the series. This term, which consists of the single second-order diagram, gives the first-order smoothing approximation that was discussed in the last section. When the Reynolds number ceases to be small, the series in its raw, untreated form is not likely to be useful, and we must resort to more sophisticated methods of series summation.

Consider the subseries, exhibited in Fig. 8(a), of the series defining the vertex function Σ. The sum of the inner parts of these diagrams formally defines a function $G_{ab}(\mathbf{k},\omega)$ called the full propagator, which we denote by a heavy line. Every diagram in Fig. 7(b) belongs to exactly one series analogous to Fig. 8(a) that can be similarly summed, and so the entire series for Σ can be rewritten in terms of G, as in Fig. 8(b). The diagrams remaining in this consolidated series are those whose arcs cannot be divided into two groups such that no member of one group intersects any member of the other.

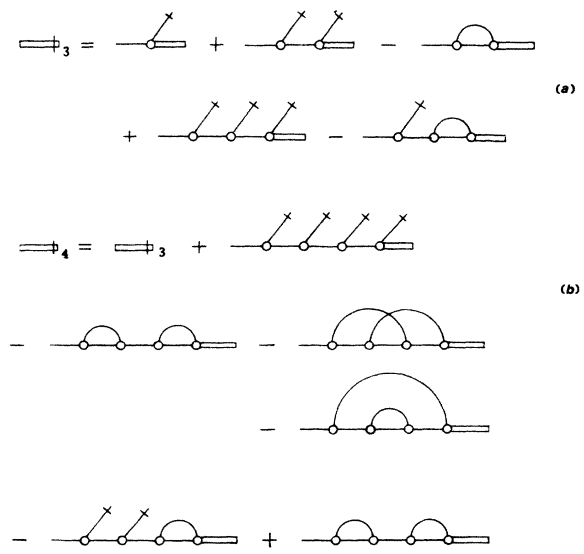

FIG. 5. Third and fourth iterations of Fig. 2(b).

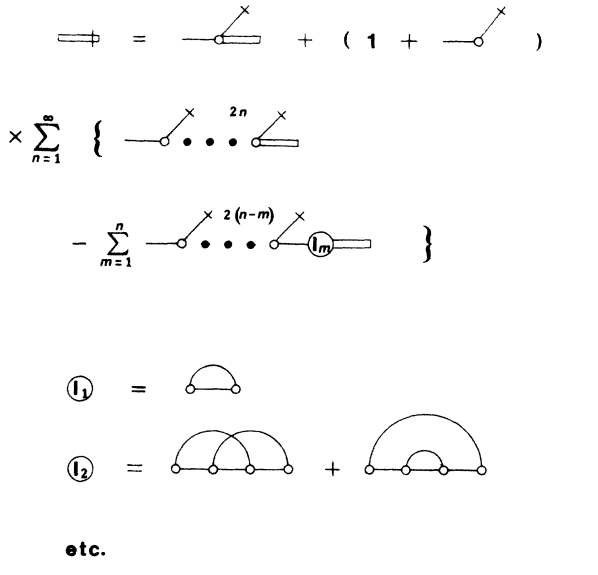

FIG. 6. Full expansion of short-wave component.

The resummation of Fig. 7(b) has not simplified the problem of calculating Σ at all; rather, we have just transformed the problem of finding Σ into the problem of finding G. But now we can perform the same resummation procedure on the series for G itself, and obtain a consolidated series for G in terms of itself, which can be expressed in closed form in terms of Σ (Fig. 9). This equation, whose algebraic form is

$$G_{ac}(\mathbf{k},\omega)=G^0(\mathbf{k},\omega)\delta_{ac}+G^0(\mathbf{k},\omega)\Sigma_{ab}(\mathbf{k},\omega)G_{bc}(\mathbf{k},\omega)\ ,$$

can be inverted:

$$G_{ab}(\mathbf{k},\omega)=[G^{0-1}(\mathbf{k},\omega)-\Sigma(\mathbf{k},\omega)]^{-1}{}_{ab}\ . \tag{4.2}$$

With G given by (4.2), Σ is now determined as the solution of a nonlinear integral equation, known as the *Dyson equation*. Truncating the Dyson equation and solving the

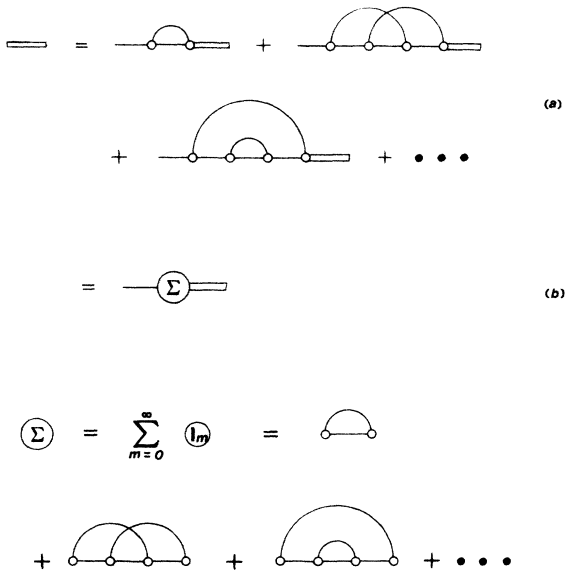

FIG. 7. Dispersion relation for long-wave component.

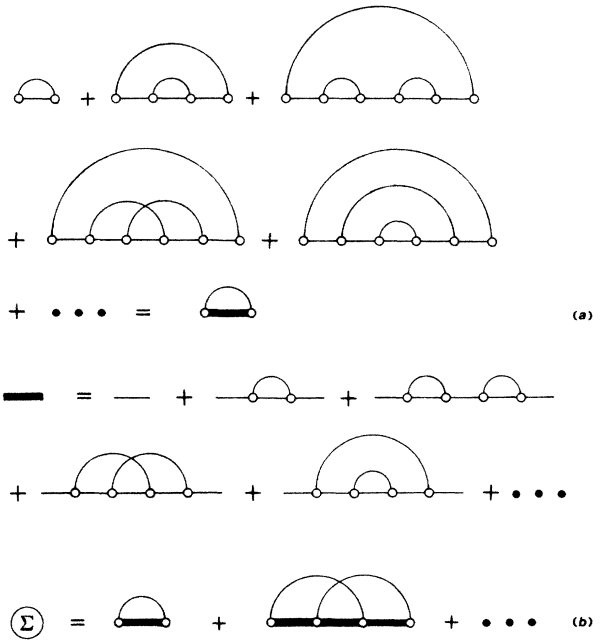

FIG. 8. Resummation of subseries.

resulting closed-integral equation gives a new approximation to the vertex, which may have useful properties that no finite number of terms of the original expansion had.

The DIA for Σ is given by the lowest truncation of the Dyson equation

$$\Sigma_{af}(\mathbf{k},\omega) = -R^2 P_{abc}(\mathbf{k}) \times \sum_{\hat{\mathbf{Q}}\in W} |A(\hat{\mathbf{Q}})|^2 (\delta_{be} - \hat{Q}_b \hat{Q}_e - i\epsilon_{bex}\hat{Q}_x) \times G_{cd}(\mathbf{k}-\hat{\mathbf{Q}},\omega) P_{def}(\mathbf{k}-\hat{\mathbf{Q}}) \quad (4.3)$$

with G_{ab} given by (4.2). By reexpanding (4.3) in powers of R, it turns out that the DIA simply consists of summing up the subset of the full diagram series that consists of all diagrams whose arcs do not intersect at all. Whether or not the DIA is a good approximation depends on the relative importance of the diagrams with less trivial topological structure; this issue will be discussed in Sec. VI.

V. RESULTS OF HIGHER-ORDER THEORY

For the simple Beltrami flow (1.2), the sum of all the diagrams of a given order n, which is of order R^n by definition, is also of order k^n in the long-wave limit. In this limit, therefore, only the single second-order diagram contributes to the dynamics of the perturbation, and hence

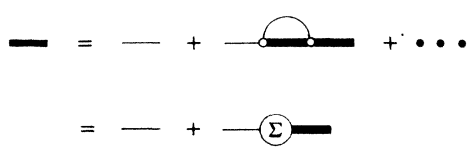

FIG. 9. Dyson equation for $G_{ab}(\mathbf{k},\omega)$.

the first-order smoothing approximation is exact for large-scale disturbances to (1.2). The results of Sec. III, in particular the prediction that the flow is unstable if $R > \sqrt{2}$, are consequently valid for all finite Reynolds numbers.

One way to demonstrate this is by an appeal to classical (Orr-Sommerfeld) stability theory. Because the velocity field (1.2) is independent of the y and z coordinates, the instability modes have the *exact* form

$$\mathbf{v}'(\mathbf{x},t) = e^{i\mathbf{k}_{OS}\cdot(\mathbf{x}-\mathbf{c}t)}(u_{OS},v_{OS},w_{OS}) ,$$

where

$$\mathbf{k}_{OS} = (0,k_2,k_3), \quad \mathbf{c} = (0,c_2,c_3) ,$$

and u_{OS},v_{OS},w_{OS} are functions of x alone. Eliminating v_{OS} and w_{OS} from the linearized Navier-Stokes equations yields an Orr-Sommerfeld equation for $u_{OS}(x)$:

$$[U(x)-c]\left[\frac{d^2u_{OS}}{dx^2} - k_{OS}^2 u_{OS}\right] - \frac{d^2U(x)}{dx^2}u_{OS} = \frac{1}{ik_{OS}R}\left[\frac{d^2}{dx^2} - k_{OS}^2\right]^2 u_{OS} , \quad (5.1)$$

where $k_{OS} = |\mathbf{k}_{OS}|$, and

$$U(x) = \mathbf{k}_{OS}\cdot\bar{\mathbf{v}}(x)/k_{OS} , \quad c = \mathbf{k}_{OS}\cdot\mathbf{c}/k_{OS}$$

are the components of $\bar{\mathbf{v}}$ and $\mathbf{c}$ parallel to $\mathbf{k}_{OS}$.

In the long-wave limit, with finite Reynolds number, the quantity $k_{OS}R$ is small, and (5.1) can be solved to give $u_{OS}(x)$ as a power series in $k_{OS}R$. But this is exactly the same procedure that we followed in Sec. IV, although here we performed more preliminary simplifications before expanding. The series obtained using either formalism must agree at each order in R; therefore the sum of all the nth-order diagrams in the diagram expansion must equal the coefficient of R^n in the Orr-Sommerfeld expansion, which is proportional to k_{OS}^n. This result can also be demonstrated directly by keeping track of the orders of successive approximations to $v_a^>$ while iterating (2.11b); we omit this calculation because the details are much more intricate and no more instructive than the Orr-Sommerfeld treatment.

The reason for the simplification of the series appears to be the fact that in a sufficiently regular flow, the long-wave perturbation modes also have regular spatial behavior. The Fourier components of the perturbation decay algebraically with wave number at any Reynolds number; indeed, they decay so rapidly that the component of the disturbance at any wave vector which is the sum of $\mathbf{k}$ and a nonzero combination of two or more basic-flow wave vectors do not participate in the dynamics. There is therefore no transfer of perturbation energy to higher and higher wave numbers, and it is not surprising that the long-wave evolution depends strongly on the molecular viscosity, even in the high-Reynolds-number limit.

For flows with complex spatial structure, the perturbation modes also have very involved spatial structure. In fact, the perturbation is likely to become singular in the limit of infinite Reynolds number. There is no finite set

of terms from the original expansion that satisfactorily describes perturbations to almost-isotropic flows at moderate or high Reynolds number. Even in the long-wave limit, all diagrams in the series [Fig. 8(b)] are nominally of order k^2, which indicates that components of the perturbation at all length scales are important in the dynamics of the long-wave part. It is reasonable to expect that a cascade may develop at high Reynolds numbers, with perturbation energy from the largest scales being transferred to smaller and smaller scales until it can be efficiently dissipated by viscosity. The damping of long-wave disturbances would then become independent of the molecular viscosity for large Reynolds numbers, and be determined by the velocity and length scales of the flow field alone.

Although the DIA does not involve anything like the complexity of the full series for Σ in Fig. 7, it nonetheless includes some of the structure of the perturbation at arbitrarily small scales. If there is an energy cascade for the perturbation, we may be able to deduce some of its qualitative characteristics by analyzing its DIA equations. The essence of the problem is to solve (4.3) for the renormalized vertex $\Sigma_{ab}(\mathbf{k},\omega)$. Since the basic flow is isotropic (to an arbitrarily good approximation), the tensors G and Σ have the forms

$$G_{ab}(\mathbf{k},\omega)=g(k,\omega)(\delta_{ab}-k_a k_b/k^2)-ih(k,\omega)\epsilon_{aby}(k_y/k) ,$$

$$\Sigma_{ab}(\mathbf{k},\omega)=\sigma(k,\omega)(\delta_{ab}-k_a k_b/k^2)+i\tau(k,\omega)\epsilon_{aby}(k_y/k) ,$$

where g, h, σ, and τ are scalar functions that depend on the wave vector $\mathbf{k}$ only through its modulus k.

Since we are primarily interested in the long-time, large-scale behavior of the Green's function, we can simplify the analysis of the integral equations by setting the frequency ω to zero within the integrals; the problem is insensitive to this approximation, and the resulting simplification is enormous. Then, by extracting the symmetric and antisymmetric parts of (4.3), respectively, we can reduce the Dyson equation to a pair of scalar integral equations over the unit sphere, which can in turn be transformed into integrals over the cosine of the angle between $\mathbf{k}$ and $\hat{\mathbf{Q}}$:

$$\sigma(k,0)=-\tfrac{1}{4}R^2\int_{-1}^{1}dc\frac{(1-c^2)}{q^2}[\alpha(k,c)g(q,0)+\beta(k,c)h(q,0)] ,$$

$$\tau(k,0)=-\tfrac{1}{4}R^2\int_{-1}^{1}dc\frac{(1-c^2)}{q^2}[\gamma(k,c)g(q,0)+\eta(k,c)h(q,0)] , \tag{5.2}$$

where the "kernels" of the integral equations are given by

$$q\equiv q(k,c)\equiv(1+k^2-2kc)^{1/2} ,$$

$$\alpha(k,c)=2kc-4k^3c+2k^4,\quad \beta(k,c)=2kc-2k^2 ,$$

$$\gamma(k,c)=4k^2c-4k^3,\quad \eta(k,c)=2k^2c-2k^3 .$$

The integral equations (5.3) are "closed" by solving Eq. (4.2) for g and h in terms of σ and τ, which yields the relations

$$g(k,\omega)=[k^2-\sigma(k,\omega)]/D(k,\omega) ,$$
$$h(k,\omega)=-\tau(k,\omega)/D(k,\omega) \tag{5.3}$$

with

$$D(k,\omega)=[k^2-\sigma(k,\omega)]^2-\tau(k,\omega)^2 .$$

Equations (5.2) and (5.3) can be solved using standard numerical techniques. The functions σ and τ are approximated by specifying their values at a suitable mesh of points on the k axis, and linearly interpolating the values for all other points. The integrals (5.3) can then be evaluated at the mesh points using a standard ten-point Gaussian scheme for the c integrals. By performing a many-dimensional Newton iteration, we can rapidly find the values of σ and τ at the mesh points which are reproduced by the integration. Successively finer meshes were used until the values for the eddy viscosity (see below) changed by 1% or less upon doubling the resolution.

It is easily checked that the asymptotic behavior of $\sigma(k,0)$ is quadratic in k as $k\to 0$, while the asymptotic behavior of $\tau(k,0)$ is cubic in k. So, although the antisymmetric part of Σ is important for the solution of the integral equation, it does not enter explicitly into the long-wave equation. The behavior of long-wave perturbations is determined by the quantity $\Gamma=\lim_{k\to 0}[-\sigma(k,0)/k^2R]$, which is a nontrivial function of the Reynolds number R. Using Eqs. (4.1) and (5.3), the long-wave dispersion relation is given by

$$-i\omega=-k^2[1+R\Gamma(R)] , \tag{5.4a}$$

or, in the original dimensional units,

$$-i\omega=-k^2[\nu+(U_{\rm rms}L)\Gamma(R)] . \tag{5.4b}$$

Thus, for large Reynolds number, a long-wave disturbance damps out as if acted on by an effective eddy viscosity $(U_{\rm rms}L)\Gamma(R)$. A plot of $\Gamma(R)$ as a function of Reynolds number is shown in Fig. 10; it should be noted that as R increases, Γ tends rapidly to a finite asymptotic value, confirming the hypothesis that at high Reynolds number, the exact value of the molecular viscosity is unimportant for the dynamics. The straight line through the origin has slope $\frac{8}{15}$, corresponding to the first-order smoothing approximation. The curve $\Gamma(R)$ is tangent to this line at the origin, confirming the result that at low Reynolds numbers, the DIA reproduces first-order smoothing.

A couple of remarks may be made about extensions of the theory beyond the case of long-wave linear perturbations. The analysis of Sec. II does not actually depend on the precise character of $\langle\ \rangle$ as the projection onto functions with support in a neighborhood of zero in wave-vector space; the formalism remains applicable if $\langle\ \rangle$ denotes the projection onto functions with support in a neighborhood of any desired wave vector. We can therefore use first-order smoothing or the DIA to investigate the behavior of a perturbation of arbitrary wave vector, although it becomes very difficult to evaluate the sums in (3.6) once k and ω become order one. When k becomes much larger than unity, corresponding to a very small-scale perturbation, the calculations again become simple. As expected, such high-wave-vector perturbations are rap-

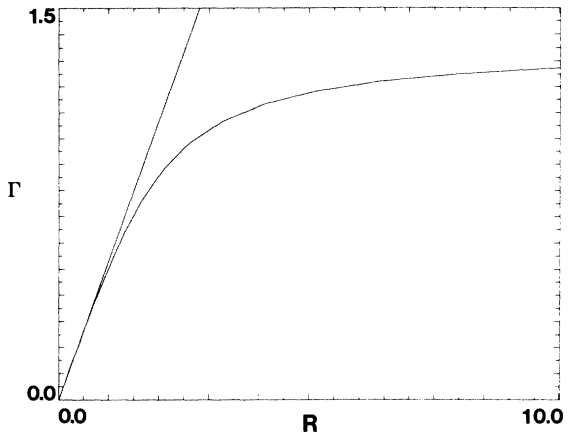

FIG. 10. Eddy viscosity factor Γ as a function of Reynolds number R.

idly dissipated by molecular viscosity, before the effect of basic flow can be felt.

We can also consider the effects of weak nonlinearity, for a perturbation of small but finite magnitude. By retaining terms of second order in the perturbation amplitude in the analysis, a quadratically nonlinear equation of motion may be obtained. The coefficient of the quadratic term can be expressed in terms of nontrivially connected diagrams, and it appears that even at this order the algebra would be too complicated to yield any information about the nonlinear dynamics. Whatever the form of the coefficient, however, it must be such as to maintain the Galilean invariance of the whole problem; that is, if a uniform translation $V_i\delta(\mathbf{k})\delta(\omega)$ is added to the long-wave velocity $v_i^<(\mathbf{k},\omega)$, the frequency ω must change to $\omega-\mathbf{k}\cdot\mathbf{V}$. This requirement alone is sufficient to determine that the quadratically nonlinear term has exactly the same form as the advective term in the basic Navier-Stokes equations; all the complicated corrections must cancel. Therefore, weakly nonlinear, large-scale perturbations to almost-isotropic Beltrami flow satisfy

$$\begin{aligned}&\partial_t\mathbf{v}^<+\mathbf{v}^<\cdot\nabla\mathbf{v}^<\approx-\nabla p^<+\nu_{\text{eff}}\nabla^2\mathbf{v}^<\ ,\\&\nu_{\text{eff}}=\nu+(U_{\text{rms}}L)\Gamma(R)\ .\end{aligned}\tag{5.5}$$

VI. DISCUSSION

We have considered the long-wave stability properties of two viscous Beltrami flow fields, which were chosen to exhibit the features of extreme isotropy versus anisotropy. To simplify the analysis, we assumed that the flows were maintained by external body forces. Although such forced flows rarely occur in the real world, this hypothesis makes it possible to construct the stability theory in an uncomplicated manner. If it were desired, our analysis could then be extended, using multiple-scale techniques, to treat more realistic problems, such as the development of large-scale structures in slowly decaying viscous flows.

For the simple Beltrami flow, the first-order smoothing approximation correctly describes the behavior of long-wave perturbations, and instability is predicted if the Reynolds number of the flow exceeds $\sqrt{2}$. For the class of almost-isotropic Beltrami flows, both the first-order smoothing and direct-interaction approximations indicate that the reaction of the basic flow enhances the damping of long-wave disturbances. At large Reynolds numbers, the DIA predicts that the damping rate should be essentially independent of the molecular viscosity, which agrees with an intuitive picture of the dynamics. Our results appear to be in some conflict with the general conclusions of Moffatt[5] and Moissev *et al.*,[6] and it is important to discover whether this conflict is real or whether it vanishes upon closer inspection of the particular problems analyzed. It turns out that our results are completely consistent with those of Moissev *et al.*[6] for highly compressible flow, the essential difference being the degree of compressibility involved; we illustrate this by repeating the first-order smoothing calculation for almost-isotropic compressible Beltrami flow in the Appendix.

Moffatt analyzes the Arnol'd-Beltrami-Childress (ABC) flow, which is a Beltrami flow in the class (1.1) with the explicit form

$$\begin{aligned}\bar{u}&=B\sin(y)+C\cos(z)\ ,\\\bar{v}&=C\sin(z)+A\cos(x)\ ,\\\bar{w}&=A\sin(x)+B\cos(y)\ ,\end{aligned}$$

where A,B,C, are real numbers. A,B,C are often chosen to be equal to unity in studies of ABC flows;[9] this choice yields a flow which is intermediate in isotropy between our simple flow and almost-isotropic flows. An indication of the *inviscid* stability or instability of the flow may be obtained by calculating Arnol'd's second variation of the kinetic energy with respect to isocirculational displacements of the fluid particles. This functional is of indefinite sign for suitably aligned long-wave perturbations with the same helicity as the basic flow, and indeed such perturbations grow with time in the initial stages of their development.[5] Moffatt's analytical results are supported by a recent numerical investigation of the stability of ABC flow in a viscous fluid at moderate Reynolds number.[10]

Despite its apparent isotropy, the ABC flow has important properties that distinguish it from the typical almost-isotropic flows investigated here. The indefiniteness of the Arnol'd functional, for example, is a property of the special orientation of the basic flow wave vectors which ceases to hold when there are more than three independent Fourier components in the flow. There are also indications that the form of Moffatt's equation of motion for long-wave perturbations, which involves the third-order differential operator $\nabla\times\nabla^2$ (hence the sensitivity to the helicity of the disturbance) gives way to a reflection-invariant form involving only a second-order operator for flows with more than three independent Fourier components. The difference between the stability properties of the ABC flow and the almost-isotropic flows may be a consequence of the difference between their topological structures. Recent investigations of the streamline structure of the ABC flow[9] show that large regions of space are occupied by streamlines with highly regular structure, while in Beltrami flows with icosahedral symmetry, for example, or more complex cubic symmetry, it appears that almost all streamlines are ergodic.[11] It seems likely

that the ABC flow has more in common with our anisotropic flow than our almost-isotropic flows, as far as its stability properties are concerned.

Although the DIA gives physically sensible results for this and other problems,[2,3] it is still an approximation. In fact, it is not even a rational approximation, in the sense that there are no indications that the omitted terms are any smaller than those retained. The most we can hope when using this technique is that it incorporate the most important physical processes sufficiently completely to give answers that are qualitatively correct. In this problem, the most important feature is probably the ability of the basic flow to mediate the transport of perturbation energy from large scales to small scales. In addition, the equations have the property that the nonlinear terms conserve the energy and helicity in the flow.

We can actually construct a model system with these essential ingredients. Imagine a large number of realizations of almost-isotropic flows, all chosen from an ensemble with well-defined statistics. We can then ask what happens if each realization is given a perturbation and then allowed to evolve according to the linearized Navier-Stokes equations; in particular, we want to know what happens to the perturbation averaged over all realizations. This situation is exactly analogous to that of the random harmonic oscillator extensively analyzed by Kraichnan.[12]

Now, consider the effect of formally coupling the dynamics of the different realizations together. The behavior will be altered, of course, with the details depending on the nature of the coupling. If the couplings are suitably restricted, however, the total energy and helicity of all the realizations taken together will still be constants of motion. The system obtained by choosing the couplings to be as random as possible within these restrictions is called the random-coupling model, and its statistical behavior is given exactly by the DIA.[12] These properties of the random-coupling model indicate that there are grounds for expecting the DIA to include at least some of the important physical effects in other systems also. indeed, for passive-scalar dispersal in reflectionally invariant turbulence the DIA and modifications thereof have been highly successful in predicting the asymptotic long-time diffusion rate.[2,4,13]

Unfortunately, the DIA does not always perform so successfully, particularly in the presence of helical effects. The predictions of passive-scalar dispersal in helical turbulence are in error by a factor of three,[3] and helicity fluctuations in conducting fluids give rise to anomalous effects in the diffusion of magnetic fields that are inaccessible by the DIA.[23] There are also indications that helicity in the flow introduces effects that do not appear at any finite order in the perturbation expansion.[4] Under these circumstances, we cannot present our findings as quantitative facts, but nonetheless, we believe that this work is an important step in understanding the dynamical properties of helical flows.

ACKNOWLEDGMENTS

While this work was in progress, we benefited greatly from the comments and criticisms of S. A. Orszag, who also provided the facilities for performing the numerical work. We are grateful to H. K. Moffatt for sending us a copy of his work on a closely related subject, prior to publication, and for his comments on a draft of this paper. The work was supported by the U. S. Office of Naval Research under Contract No. N00014-85-K-0201 and the U. S. Air Force Office of Scientific Research under Contract No. F49620-85-C0026. B. J. B. also thanks the National Science Foundation for financial support.

APPENDIX: INSTABILITY IN ISOTROPIC COMPRESSIBLE FLOW

Beltrami flows, in particular the family (1.1), are also exact solutions of the Euler equations in an isentropic, compressible fluid, and can be maintained by a suitable external agency in a viscous compressible fluid. In order to investigate the effects of compressibility on the possible generation of large-scale motions, it is simplest at first to ignore the influence of pressure forces on the dynamics of the short-wave part of the perturbation. This approximation is crucial to the analysis of Moissev *et al.*,[6] who nonetheless retain the pressure in the long-wave component. For consistency, we shall neglect the perturbation pressure in all its manifestations and obtain essentially the same results.

If we neglect the perturbation pressure field (and drop the incompressibility condition, of course), the analysis of long-wave disturbances proceeds exactly as in Sec. II. The only difference is that the tensor through which two velocity components interact no longer depends only on their sum, but on their individual wave numbers

$$P'_{abc}(\mathbf{k}^1,\mathbf{k}^2)=k_c^1\delta_{ab}+k_b^2\delta_{ac}\ . \tag{A1}$$

This tensor is no longer symmetric in b,c, which is the crucial feature allowing the long-wave instability. Using the first-order smoothing approximation we obtain the following equation, which is analogous to (3.3), for the evolution of a long-wave perturbation:

$$v_a^<(\mathbf{k},\omega)=-R^2G^0(\mathbf{k},\omega)v_e^<(\mathbf{k},\omega)\sum_{\hat{\mathbf{Q}}\in W}[\,|A(\hat{\mathbf{Q}})|^2P'_{abc}(\hat{\mathbf{Q}},\mathbf{k}-\hat{\mathbf{Q}})G^0(\mathbf{k}-\hat{\mathbf{Q}},\omega)(\delta_{bd}-\hat{Q}_b\hat{Q}_d-i\epsilon_{bdx}\hat{Q}_x)P'_{cde}(-\hat{\mathbf{Q}},\mathbf{k})]\ . \tag{A2}$$

For an almost-isotropic flow, evaluating the right-hand side in the long-wave limit gives

$$v_a^<(\mathbf{k},\omega)=\tfrac{2}{3}R^2G^0(\mathbf{k},\omega)\epsilon_{abc}ik_bv_c^<(\mathbf{k},\omega)+O(k^2)\ ,$$

or, in the space-time domain,

$$\partial_t\mathbf{v}^<=\tfrac{2}{3}R^2\nabla\times\mathbf{v}^<+O(\nabla^2)\ , \tag{A3}$$

which predicts instabilities in the form of large-scale helical flows with helicity in the same sense as the basic flow.[5,6]

[1]G. Sivashinsky and Y. Yakhot, Phys. Fluids **28**, 1040 (1985).
[2]R. H. Kraichnan, J. Fluid Mech. **75**, 657 (1976); **77**, 753 (1976).
[3]R. H. Kraichnan, J. Fluid Mech. **81**, 385 (1977).
[4]I. T. Drummond, S. Duane, and R. R. Horgan, J. Fluid Mech. **138**, 75 (1984).
[5]H. K. Moffatt, J. Fluid Mech. (to be published).
[6]S. S. Moissev, R. Z. Sagdeev, A. V. Tur, G. A. Khomenko, and V. V. Yanovskii, Zh. Eksp. Teor. Fiz. **85**, 1979 (1983) [Sov. Phys.—JETP 58, 1149 (1983)].
[7]R. B. Pelz, V. Yakhot, S. A. Orszag, L. Shtilman, and E. Levich, Phys. Rev. Lett. **54**, 2505 (1985).
[8]H. K. Moffatt, J. Fluid Mech. **159**, 359 (1985).
[9]T. Dombre, U. Frisch, J. M. Greene, M. Henon, A. Mehr, and A. M. Soward, J. Fluid Mech. (to be published).
[10]D. Galloway and U. Frisch (unpublished).
[11]B. J. Bayly (unpublished).
[12]R. H. Kraichnan, J. Math. Phys. **2**, 124 (1960).
[13]R. Phythian and W. C. Curtis, J. Fluid Mech. **89**, 241 (1978).